Journal of Earth Science, *Vol. 25*, *No. 5*, *p. 779–786*, *October 2014* *ISSN 1674-487X*
Printed in China
DOI: 10.1007/s12583-014-0472-0

Conodont Biostratigraphy across the Permian-Triassic Boundary at the Xinmin Section, Guizhou, South China

Ning Zhang*[1], Haishui Jiang*[2], Wenli Zhong[1], Haohao Huang[1], Wenchen Xia[1]
1. *Faculty of Earth Sciences*, *China University of Geosciences*, *Wuhan* 430074, *China*
2. *State Key Laboratory of Biogeology and Environmental Geology*, *China University of Geosciences*, *Wuhan* 430074, *China*

ABSTRACT: A continuous sedimentation at the Xinmin Section, Anshun, Guihzou Province, with the Upper Permian Talung Formation dominated by bedded siliceous rocks, and the Lower Triassic Luolou Formation consisting mudstones and marls as well as siliceous mudstones at its basal part indicates that it represents a deeper-water basinal facies across the Permian-Triassic boundary. Based on a systematic conodont biostratigraphic work, nine conodont species belong to two genera have been identified in this study. It enable us to establish five conodont zones at this section, in ascending order, they are: *Clarkina changxingensis* Zone (beds 1-3–4-2), *Clarkina yini* Zone (beds 4-3–5-1-1), *Clarkina meishanensis* Zone (beds 5-1-2–5-2), *Hindeodus changxingensis* Zone (beds 5-3-1–5-3-2) and *Hindeodus parvus* Zone (beds 5-3-3–5-3-4), respectively. According to the first occurrence of *Hindeodus parvus* in bed 5-3-3, the Permian-Triassic boundary is placed at the base of bed 5-3-3. This conodont zonation of the Xinmin Section provides precise biostratigraphic framework for further investigations on the geological events across the Permian-Triassic boundary at this section. In addition, the new conodont data also reveals that several siliceous beds occurred at the basal Triassic. It provides an exception of Early Triassic Chert Gap.

KEY WORDS: Permian-Triassic, conodont, Xinmin Section, Early Triassic chert.

0 INTRODUCTION

According to the comparison among conodont zones from more than twenty Permian-Triassic boundary (PTB) sections in South China, combining with isotopic records from some of these sections, Yin et al. (2013) demonstrated that a widespread end-Permian regression took place in South China and could be related with causes of the mass extinction. In this regression, most of the Yangtze carbonate platform and isolated carbonate platforms were exposed and experienced sedimentary hiatus (Yin et al., 2013). Deeper-water basinal facies section has the advantage of recording complete information across the PTB. In Hunan-Guizhou-Guangxi Basin, bedded siliceous rocks representing a deeper-water basinal facies spread widely on the top of Upper Permian. Among this kind of deep water sections, only few received detailed conodont study. By far, numerous researches had been conducted on the Dongpan Section, Guangxi (e.g., Luo et al., 2008; Feng et al., 2007; He et al., 2007). The first appearance of conodont *Hindeodus parvus* marking the base of Triassic (Yin et al., 2001), is also very important to define the PTB at basinal facies sections. However, the conodonts from two beds of lense-like limestone in the Talung Formation belonging to *Neogondolella yini* (=*Clarkina yini*) Zone (Luo et al., 2008), are not enough to precisely define the PTB at the Dongpan Section. Progresses have been made on the Bianyang Section, Guizhou Province recently. On this basinal margin section, with detailed conodont zonation, the PTB has been defined at the base of bed 6 with the first occurrence of *Hindeodus paruvs* (Yan et al., 2013).

The Xinmin Section is located at Xinmin valley, Puding County, Guizhou Province, South China (Fig. 1) and is easily accessible, well exposed, and displays a continuous sedimentation from the thin-bedded siliceous mudstone in the Talung Formation and mudstone in the Luolou Formation, indicating a deep water basinal facies. Previously, primary works have been carried on the adjacent area of this section. Yao et al. (1980) have found abundant ammonoids, gastropods, brachiopods and foraminifers at the Jiaozishan Section, which is about 4 km south to Xinmin. Research on Guizhou stratigraphy (Dong, 1997) showed that ammonoid *Pseudotirolites* is common in the Talung Formation in this area, associated with brachiopods, bivalves, gastropods, trilobites and fossil plants. Recently, many researches related to the end-Permian event were focused on the Xinmin Section. Feng et al. (2011) first described the strata across the PTB and reported trilobite *Pseudophillip* sp. from the top of Changhsingian at this section. Hu et al. (2012, 2011) found organic carbon isotope exhibited a distinct negative shift in bed 5. According to the magnetic susceptibility curve and combining with some geochemistry index, Xu et al. (2012) figured out three paleoclimatic stages across the PTB. Based on geochemistry works, Shen et al. (2013, 2012)

*Corresponding author: zhangn@cug.edu.cn;
jiangliuis@163.com

Manuscript received March 18, 2014.
Manuscript accepted June 15, 2014.

Zhang, N., Jiang, H. S., Zhong, W. L., 2014. Conodont Biostratigraphy across the Permian-Triassic Boundary at the Xinmin Section, Guizhou, South China. *Journal of Earth Science*, 25(5): 779–786. doi:10.1007/s12583-014-0472-0

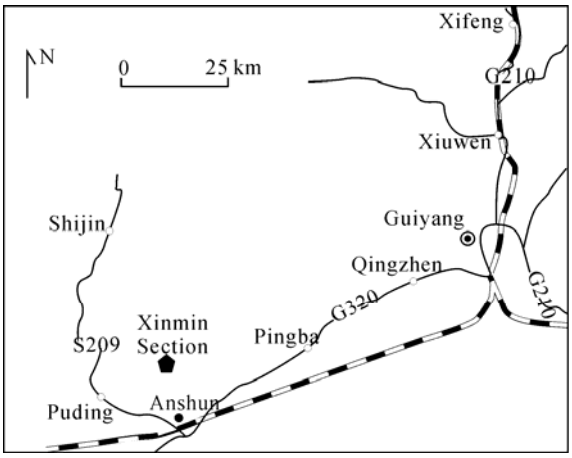

Figure 1. Map showing the location of the Xinmin Section.

discussed the volcanism records at this section. Conodont biostratigraphy at this section were literally reported (without conodont image illustration, e.g., Shen et al. (2013, 2012), Xu et al. (2012), Feng et al. (2011), Hu et al. (2011). Xu et al. (2012) have reported that *Hindeodus parvus* in the upper part of bed 5-3, suggesting that the PTB should be placed in bed 5-3. Unfortunately, conodonts have never been illustrated in these references leading to the PTB at the section incredible. During the past 4 years, we carried out intensive conodont biostratigraphic works at the Xinmin Section. Hereby, we provide the first-hand conodont data to define the PTB at this section. This will be helpful to improve correlations among basinal sections and sections from other facies and promote the research in the basinal facies sections of the PTB.

1 MATERIALS AND METHOD

In this study, 46 conodont samples (about 4 kg for each sample) were collected from the uppermost Permian and lowermost Triassic (beds 1–6) of the Xinmin Section. The bed numbers used in this paper are the revised numbers of Shen et al. (2013, 2012), Xu et al. (2012) and Feng et al. (2011) (see Fig. 2). Thickness of each bed is showing in Figure 2. For sampling, bed 5-1 (0.1 m in thickness) has been divided into 3 sub-beds, respectively 5-1-1 (0.02 m), 5-1-2 (0. 04 m) and 5-1-3 (0.04 m); bed 5-3 (0.24 m in thickness) has been divided into 4 sub-beds, respectively 5-3-1 (0.08 m), 5-3-2 (0.08 m), 5-3-3 (0.03 m) and 5-3-4 (0.05 m). Limestone samples have been processed by acetic acid dissolution procedure (see Jiang et al., 2007). Mudstone and clay samples were first processed by 10% acetic acid dissolution procedure, then soaking in water. Siliceous rock samples were processed by 5% hydrofluoric acid dissolution procedure, collecting residues per 24 h. Conodont separation method is the same with Jiang et al. (2007).

2 CONODONT BIOSTRATIGRAPHY

For the first time, useful conodonts have been found from the Permian-Triassic transition interval of the Xinmin Section (Plate 1 and Plate 2). Their occurrences and distribution in each bed or sub-bed are shown in Fig. 2. These data enable us to establish five important conodont zones across the PTB at this section, in ascending order, they are: *Clarkina changxingensis* Zone, *Clarkina yini* Zone, *Clarkina meishanensis* Zone, *Hindeodus changxingensis* Zone and *Hindeodus parvus* Zone respectively.

***Clarkina changxingensis* Zone (beds 1-3–4-2)**

Lower limit: First occurrence of *C. changxingensis*.

Upper limit: First occurrence of *C. yini*.

Associated taxa: *C. wangi*, C. *postwangi*, *C.* sp.. Previously, Hu et al. (2011) assigned beds 1–2 to *C. postwangi* Zone. Xu et al. (2012) assigned beds 1–2 and the base of bed 3 to *C. zhangi* Zone. However, both zones lack basic description and have never been formal reported before. Shen et al. (2012) assigned beds 1–2 to *C. changxingensis*-*C. postwangi* assemblage zone. It must be point out that a more precise and correlatable conodont zone is normally named by a single species with the first appearance of the key species marking the lower or upper limit of the zone, especially in researches on the Permian-Triassic transition, e.g., Jiang et al. (2011, 2007), Shen and Mei. (2010). Conodont assemblage zone was reported before, for example, Zhang et al. (2009) reported the *C. changxingensis*-*C. deflecta* asemblage zone and *C. yini*-*C. zhangi* asemblage zone, but *C. changxingensis*-*C. postwangi* assemblage zone has never been reported.

***Clarkina yini* Zone (beds 4-3–5-1-1)**

Lower limit: First occurrence of *C. yini*.

Upper limit: First occurrence of *C. meishanensis*.

Associated taxa: *C.* sp.. The species *C. yini* was established based on the specimen from the top of Changxingian at Meishan, Zhejiang (Mei et al., 1998). Mei et al. (1998) first established *C. yini*-*C. zhangi* assemblage zone at the Meishan Section. Later, it was replaced by *Clarkina yini* Zone by Yin et al. (2001). Hu et al. (2011) assigned bed 3 and the lower part of bed 4 to this zone. While Xu et al. (2012) put most part of bed 3 and bed 4 to this zone. Shen et al. (2012) considered that strata from base of bed 3 to the middle part of bed 5 belong to this zone. As we mentioned above, all these biostratigraphic data are lack of conodont figures. Hu et al. (2011) also reported *Clarkina hauschkei* Zone in bed 4 at this section. There is some controversy about this species and this zone (Jiang et al., 2007, p. 50 therein), and we have not found any specimens similar to *C. hauschkei* based on our careful checking on all specimens.

***Clarkina meishanensis* Zone (beds 5-1-2–5-2)**

Lower limit: First occurrence of *C. meishanensis*.

Upper limit: First occurrence of *H. changxingensis*.

Associated taxa: *C. changxingensis*, *C. tulongensis*, *C.* sp. *A* (Jiang), *C.* sp., *H.* sp.. Species *C. meishanensis* was established in Zhang et al. (1995). Later, Mei et al. (1998) first established this zone at the Meishan section. Hu et al. (2011) assigned beds 5a–5b (comparable to beds 5-1–5-3 in this study) to this zone. Xu et al. (2012) put the upper part of bed 4 and lower part of bed 5 to this zone. While Shen et al. (2012) put the upper part of bed 5 and bed 6 to this zone.

***Hindeodus changxingensis* Zone (beds 5-3-1–5-3-2)**

Lower limit: First occurrence of *H. changxingensis*.

Upper limit: First occurrence of *H. parvus*.

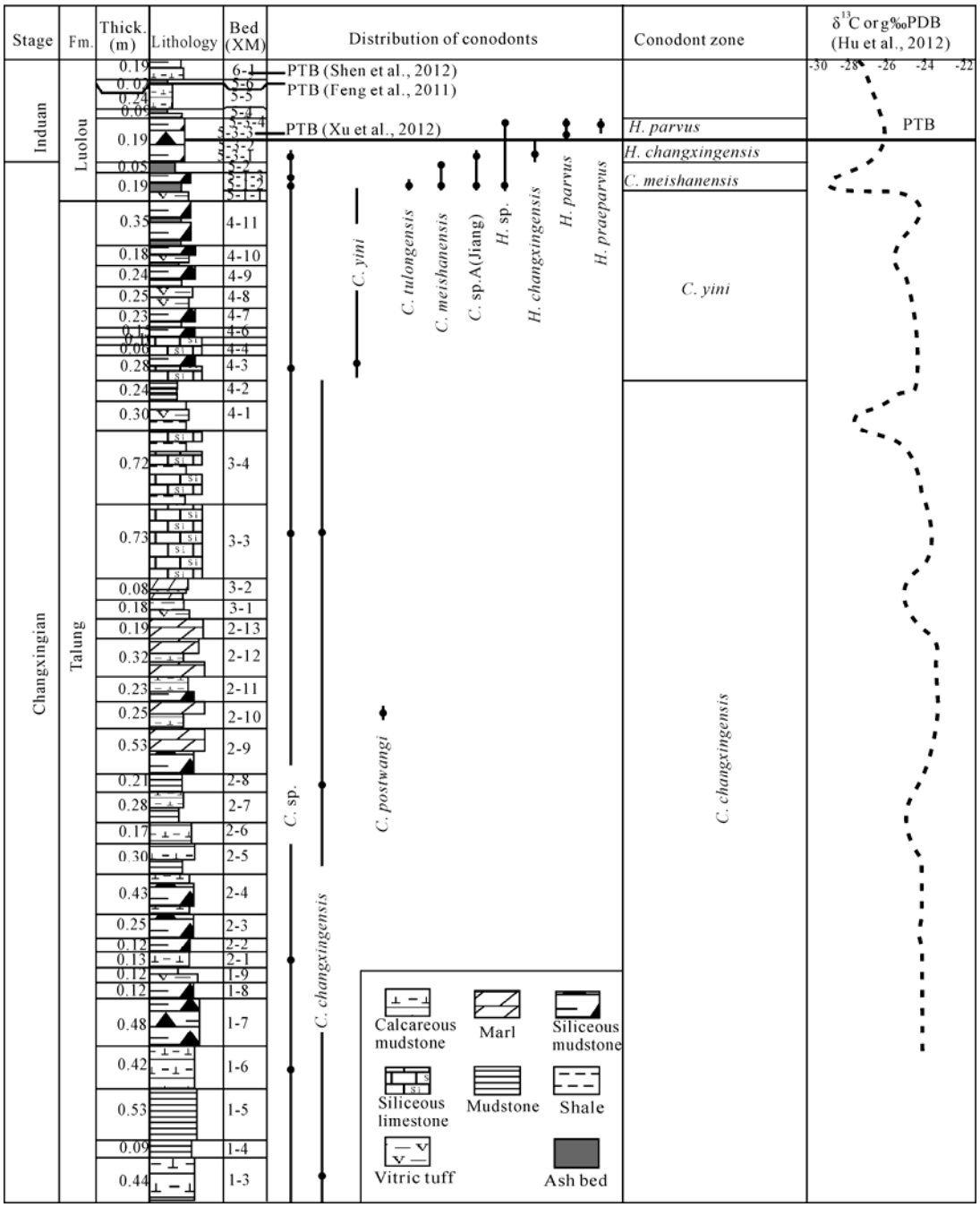

Figure 2. Lithology, conodont ranges and zonations across the PTB in the Xinmin Section.

Associated taxa: *C. changxingensis*, *C. meishanensis*, *C.* sp. *A* (Jiang), *C.* sp.. Previously, this zone has been reported at Meishan, Zhejiang (Zhang et al., 2009; Jiang et al., 2007), Shangsi, Sichuan (Jiang et al., 2011), Yangou, Jiangxi (Sun et al., 2012), Bianyang, Guizhou (Yan et al., 2013). The significances of the first appearance of *H. changxingensis* or the zone have been discussed respectively (Jiang et al., 2011; Metcalfe et al., 2007). The first establishment of *H. changxingensis* Zone at Xinmin made it could be better correlated to the sections mentioned above.

***Hindeodus parvus* Zone (beds 5-3-3–5-3-4)**

Lower limit: First occurrence of *H. parvus*.

Upper limit: No conodont specimen has been found above bed 5-3-4. We currently define the top of this zone in terms of ranges of species of *H. parvus*. So the upper limit of this zone is tentatively placed at the top of bed 5-3-4. It is possible that the *Hindeodus parvus* Zone extends above the bed 5-3-4.

Associated taxa: *H. praeparvus*, *H.* sp.. Xu et al. (2012) assigned the upper part of bed 5-3 and the above beds to this zone. According the reliable *H. parvus* specimens in this study, we precisely defined the first appearance datum of this key species and the PTB, which located at the base of bed 5-3-3.

3 DISCUSIONS

3.1 The PTB at the Xinmin Section

Although lacking image illustration of any conodont speimens, the PTB at the Xinmin Section has been defined in

different horizons in previous studies. According to the occurrence of conodont *Clarkina meishanensis* and bivalve *Claraia primitiva* in bed 5-3, ammonoid *Ophiceras* sp. in bed 6-2, Feng et al. (2011) presumed the PTB at the base of bed 5-6 (Fig. 2). Xu et al. (2012) have put the PTB in bed 5-3 based on the appearance of *H. parvus* in the upper part of this bed (Fig. 2). This is close to the PTB defined in this paper. Nevertheless, Shen et al. (2012) still presumed the PTB at the base of bed 6-2 (Fig. 2).

The organic carbon isotope exhibited a distinct negative shift in the lower part bed 5 (Hu et al., 2012, comparable to beds 5-3-1 in this paper) (Fig. 2). Such a negative shift occurred in *Hindeodus changxingensis* Zone, consistent with the pattern around the PTB at Meishan (Cao et al., 2008), implying the end-Permian mass extinction boundary was probably at this horizon. This extinction boundary has been assigned in bed 5 (Shen et al., 2012, comparable to bed 5-5-1 in this paper) or at the base of bed 6 (Shen et al., 2013). After checking the order of references citation, we guess Shen et al. (2013) was earlier accepted but published later. Both mass extinction boundaries (Shen et al., 2013, 2012) are higher than the PTB defined in this study. But further detailed researches on various fossil faunas need to be carried out to define the extinction boundary.

The PTB is unmatched with the first appearance of *H. parvus* in some sections. At Shangsi Section, for example, the PTB is lower than the first appearance of *H. parvus* by consulting to mass extinction boundary, carbon isotope, occurences of key ammonoids and first occurrence of Early Triassic conodont *Isarcicella* (Jiang et al., 2011). In contrast, at Zhongzhai, Guizhou, Zhang et al. (2014) recently put the PTB above the first appearance of *H. parvus* by consulting to carbon isotope and the U-Pb age dating, and proposed that the first occurrences of *Hindeodus parvus* are diachronous in different sections. To precisely define the PTB at Zhongzhai Section and checking the only exceptional case where the *Hindeodus parvus* occurred in the Late Permian, more works on detailed fossil records including the conodont fauna need to be conducted at the Zhongzhai Section. However, considering conodont data and carbon isotopic pattern, we suppose that the first appearance of *H. parvus* is the reliable index for determining the PTB at the Xinmin Section, which defined at the base of bed 5-3-3 (Fig. 2).

3.2 Comparison with Other Sections in South China

Previously, parallel gondolellid zones and hindeodid zones have been established at both Meishan (Jiang et al., 2007) and Shangsi (Jiang et al., 2011) sections, which have the most complete conodont biostratigraphic sequences during the Permian-Triassic interval. According the first appearances of the key conodonts, Zhang et al. (2009) arranged these zones in one order, in ascending order, ther are: *C. yini* Zone, *C. meishanensis* Zone, *H. changxingensis* Zone, *C. taylorae* Zone, *H. parvus* Zone, *I. staeschei* Zone and *I. isarcica* Zone. Based on this order, Sun et al. (2012) defined a detailed conodont biostratigraphy at the Yangou Section, Leping, Jiangxi, only with absence of *Clarkina meishanensis* Zone. After minor revision, Yin et al. (2013) compared the conodont zones across the PTB among over twenty sections in South China by this one order zonation scheme.

Comparably, we think beds 4-3–5-1-1 (*Clarkina yini* Zone) at Xinmin correspond to bed 24 at Meishan (Jiang et al., 2007), bed 26 at Shangsi (Jiang et al., 2011), bed 3 at Bianyang (Yan et al., 2013), beds 19–20 at Yangou (Sun et al., 2012). Beds 5-1-2–5-2 (*Clarkina meishanensi* Zone) at Xinmin correspond to bed 25 at Meishan (Jiang et al., 2007), bed 27 to lower part of bed 28a at Shangsi (Jiang et al., 2011). Beds 5-3-1–5-3-2 (*Hindeodus changxingensis* Zone) at Xinmin correspond to beds 26–27b at Meishan (Jiang et al., 2007), the upper part of bed 28a to bed 29b at Shangsi (Jiang et al., 2011), beds 4–5 at Bianyang (Yan et al., 2013), beds 21-1–21-3 at Yangou (Sun et al., 2012). And beds 5-3-3–5-3-4 (*Hindeodus parvus* Zone) at Xinmin correspond to beds 27c–27d at Meishan (Jiang et al., 2011, 2007), beds 29c to 30a at Shangsi (Jiang et al., 2011), bed 6 at Bianyang (Yan et al., 2013), beds 21-4–24 at Yangou (Sun et al., 2012).

Jiang et al. (2011) discussed the significance of *Hindeodus changxingensis* Zone, concluding that the absence of this zone probably indicates a hiatus at the PTB section. They supposed that the Great Bank of Guizhou isolated platform was exposed at the end of Permian, which caused a disconformity around the extinction level. And this was supported by later researches (Jiang et al., 2014; Yin et al., 2013). From the comparison above, there is a complete conodont biostratigraphis sequence at the Xinmin Section and could be well correlated with other PTB sections. The complete conodont zones at this basinal facies section will contribute to better discussing the records of geological events during the Permian-Triassic transition.

3.3 Early Triassic Silicious Deposition at Xinmin

Biogenic silicious depositions from the Middle Permain to Late Permian have been reported in the northwest magin of Pangea or even worldwide (Beauchamp and Baud, 2002; Murchey and Jones, 1992). This Permian Chert Event (PCE) was caused by the end-Permian mass extinction. The dropdown of radiolarian or sponge spicule productions restrained the formation of silicious rocks in this event and that caused PCE to the end (Racki, 2003, 1999; Beauchamp and Baud, 2002; Isozaki, 1997). Following the Early Triassic Chert Gap, silicious depositions recovered from the Anisian. During past years, Early Triassic silicious depositions have been reported at some pelagic sections in New Zealand (Takemura et al., 2002; Yamakita et al., 1999) and Japan (Sano et al., 2010; Takahashi et al., 2009; Kakuwa, 1996). Recently Yang et al. (2012) firstly found a Griesbachian chert at the Gaimao Section, Guizhou, in Tethys area.

At Xinmin Section, silicious mudstone is recognized above the PTB at bed 5-3-4 and bed 6-1 above the PTB (Fig. 3). Numerous silicious mineral-agates are observed in thin sections under polarizing microscope (Fig. 4). However, further work on checking the genesis of silicious sediments at basal Triassic at this section should be carried for in discussing the Early Triassic Chert Gap event. Even so, the new finding proved that the exception of Early Triassic Chert Gap did occurred in Tethys area in addition to the Gaimao Section.

4 CONCLUSIONS

Based on our first-hand conodont materials at the Xinmin Section, five conodont zones are established. According to the first occurrence of *Hindeodus parvus*, the PTB is placed at the base of bed 5-3-3. The established conodont biostratigraphic scheme at Xinmin section provides a precise comparison with that of other PTB sections, and will be helpful for further investigating and understanding on the geological events across the Permian-Triassic boundary. The siliceous rocks occurred at bed 5-3-4 and bed 6-1 above the PTB at the Xinmin Section also provides a new example of Early Triassic siliceous sediments in Tethys area.

Figure 3. Outcrops showing silicious depositions of the Early Triassic in the Xinmin Section.

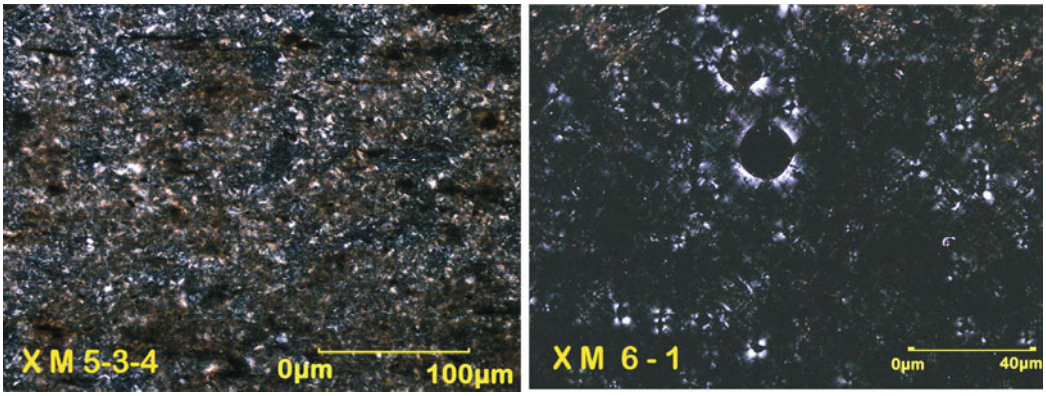

Figure 4. Thin sections showing agates in bed 5-3-4 and bed 6-1 in the Xinmin Section (under polarizing microscope).

ACKNOWLEDGMENTS

This work was supported by the Natural Science Foundation of China (Nos. 41372039, 41272044, 41172024), the 'Fundamental Research Funds for the Central Universities, China University of Geosciences (Wuhan)'. The authors also thank Prof. Xulong Lai for his thoughtful comments on this study. Thanks are also due to Jinling Yuan, Muhui Zhang and Bo Yang for their help in field sampling or in laboratory conodonts separation. All SEM pictures were taken at the State Key Laboratory of Geological Processes and Mineral Resources (China). We thank two anonymous reviewers for their helpful comments and constructive suggestions.

REFERENCES CITED

Beauchamp, B., Baud, A., 2002. Growth and Demise of Permian Biogenic Chert along Northwest Pangea: Evidence for End-Permian Collapse of Thermohaline circulation. *Palaeogeography, Palaeoclimatology, Palaeoecology*, 184(1–2): 37–63

Cao, C. Q., Wang, W., Liu, L. J., et al., 2008. Two Episodes of ^{13}C-Depletion in Organic Carbon in the Latest Permian: Evidence from the Terrestrial Sequences in Northern Xinjiang, China. *Earth and Planetary Science Letters*, 270: 251–257

Dong, W. P., 1997. Lithostratigraphy of Guizhou Province. China University of Geosciences (Wuhan) Publishing House, Wuhan. 198–211 (in Chinese with English Abstract)

Feng, F. B., Hu, Q., Feng, Q. L., 2011. Trilobite from Uppermost Changxingian in Anshun, Guizhou Province. *Journal of Stratigraphy*, 35(3): 295–298 (in Chinese with English Abstract)

Feng, Q. L., He, W. H., Gu, S. Z., et al., 2007. Radiolarian Evolution during the Latest Permian in South China. *Global and Planetary Change*, 55: 177–192

He, W. H., Feng, Q. L., Weldon, E. A., et al., 2007. A Late Permian to Early Triassic Bivlaves Fauna from the Dongpan Section, Southern Guangxi, South China. *Journal of Paleontology*, 81(5): 1009–1019

Hu, Q., Cao, J., Huang, J.H., et al., 2011. Variation of Organic Carbon Isotope and Bio-Geochemical Significances across the Permian-Triassic Boundary at Xinmin Section, Guizhou, South China. *Geological Review*, 57(3): 305–315 (in Chinese with English Abstract)

Hu, Q., Shen, J., Feng, Q. L., 2012. Variations of Carbon Isotope and the Significance of Organic Carbon Burial in the Late Permian at Xinmin Section, Guizhou Province. *Acta Sedimentologica Sinica*, 30(5): 806–816 (in Chinese with English Abstract)

Isozaki, Y., 1997. Permo-Triassic Boundary Superanoxia and Strati-

fied Superocean; Records from Lost Deep Sea. *Science*, 276: 235–238

Jiang, H. S., Lai, X. L., Luo, G. M., et al., 2007. Restudy of Conodont Zonation and Evolution across the P/T Boundary at Meishan Section, Changxing, Zhejiang, China. *Global and Planetary Change*, 55: 39–55

Jiang, H. S., Lai, X. L., Yan, C. B., et al., 2011. Revised Conodont Zonation and Conodont Evolution across the Permian-Triassic Boundary at the Shangsi Section, Guangyuan, Sichuan, South China. *Global and Planetary Change*, 77(3–4): 103–115

Jiang, H. S., Lai, X. L., Sun, Y. D., et al., 2014. Permian-Triassic Conodonts from Dajiang (Guizhou, South China) and Their Implication for the Age of Microbialite Deposition in the Aftermath of the End-Permian Mass Extinction. *Journal of Earth Scieces*, 25(3): 413–430

Kakuwa, Y., 1996. Permian-Triassic Mass Extinction Event Recorded in Bedded Chert Sequence in Southwest Japan. *Palaeogeography*, *Palaeoclimatology*, *Palaeoecology*, 121: 35–51

Luo, G. M., Lai, X. L., Feng, Q. L, et al., 2008. End-Permian Conodont Fauna from Dongpan Section: Correlation between the Deep and Shallow-water Facies. *Science in China Series D*: *Earth Sciences*, 51(11): 1611–1622

Mei, S. L., Zhang, K. X., Wardlaw, B. R., 1998. A Refined Zonation of Changhsingian and Griesbachian Neogondolellid Conodonts from the Meishan Section, Candidate of the Global Stratotype Section and Point of the Permian-Triassic Boundary. *Palaeogeography*, *Palaeoclimatology*, *Palaeoecology*, 143: 213–226

Metcalfe, I., Nicoll, R. S., Wardlaw, B. R., 2007. Conodont Index Fossil *Hindeodus changxingensis* Wang Fingers Greatest Mass Extinction Event. *Palaeoworld*, 16: 202–207

Murchey, B. L., Jones, D. L., 1992. A Mid-Permian Chert Event; Widespread Deposition of Biogenic Siliceous Sediments in Coastal, Island Arc and Oceanic Basins. *Palaeogeography*, *Palaeoclimatology*, *Palaeoecology*, 96: 161–174

Racki, G., 1999. Silica-secreting Biota and Mass Extinctions; Survival Patterns and Processes. *Palaeogeography*, *Palaeoclimatology*, *Palaeoecology,* 154: 107–132

Racki, G., 2003. End-Permian Mass Extinction: Oceanographic Consequences of Double Catastrophic Volcanism. *Lethaia*, 36: 171–173

Sano, H., Kuwahara, K., Yao, A., et al., 2010. Panthalassan Seamount-Associated Permian-Triassic Boundary Siliceous Rocks, Mino Terrane, Central Japan. *Paleontological Research*, 14: 293–314

Shen, J., Algeo, T., Hu, Q., et al., 2013. Volcanism in South China during the Late Permian and Its Relationship to Marine Ecosystem and Environmental Changes. *Global and Planetary Change*, 105: 121–134

Shen, J., Algeo, T., Hu, Q., et al., 2012. Negative C-Isotope Excursions at the Permian-Triassic Boundary Linked to Volcanism. *Geology*, 40(11): 963–966

Shen, S. Z., Mei, S. L., 2010. Lopingian (Late Permian) High-Resolution Conodont Biostratigraphy in Iran with Comparison to South China Zonation. *Geological Journal*, 45: 135–161

Sun, D. Y., Tong, J. N., Xiong, Y. L., et al., 2012. Conodont Biostratigraphy and Evolution across Permian-Triassic Boundary at Yangou Section, Leping, Jiangxi Province, South China. *Journal of Earth Science*, 23(3): 311–325

Takahashi, S., Yamakita, S., Suzuki, N., et al., 2009. High Organic Carbon Content and a Decrease in Radiolarians at the End of the Permian in a Newly Discovered Continuous Pelagic Section: A Coincidence? *Palaeogeography*, *Palaeoclimatology*, *Palaeoecology*, 271: 1–12

Takemura, A., Aita, Y., Hori, R. S., et al., 2002. Triassic Radiolarians from the Ocean-Floor Sequence of the Waipapa Terrane at Arrow Rocks, Northland, New Zealand. *New Zealand Journal of Geology and Geophysics*, 45: 289–296

Xu, G. Z., Feng, F. B., Lei, Y., et al., 2012. Variations of the Magnetic Susceptibility across the P-T Boundary at Xinmin Section in Anshun, Guizhou and Their Paleoclimatic Implications. *Acta Sedimentologica Sinica*, 30(5): 817–824 (in Chinese with English Abstract)

Yamakita, S., Kadota, N., Kato, T., et al., 1999. Confirmation of the Permian/Triassic Boundary in Deep Sea Sedimentary Rocks; Earliest Triassic Conodonts from Black Carbonaceous Claystone of the Ubara Section in the Tamba Belt, Southwest Japan. *Journal of the Geological Society of Japan*, 105: 895–898

Yan, C. B., Wang, L. N., Jiang, H. S., et al., 2013. Uppermost Permian to Lower Triassic Conodonts at Bianyang Section, Guizhou, South China. *Palaios*, 28: 509–522

Yang, B., Lai, X. L., Wignall, P. B., et al., 2012. A Newly Discovered Earliest Triassic Chert at Gaimao Section, Guizhou, Southwestern China. *Palaeogeography*, *Palaeoclimatology*, *Palaeoecology*, 344–345: 69–77

Yao, Z. Q., Xu, J. T., Zheng, Z. G., et al., 1980. Late Permian Biostratigraphy and Problem of the Permian-Triassic Boundary in Western of Guihzou and Eastern Yunnan. Science Press, Beijing. 1–70 (in Chinese with English Abstract)

Yin, H. F., Zhang, K. X., Tong, J. N., et al., 2001. The Global Stratotype Section and Point (GSSP) of the Permian-Triassic Boundary. *Episodes*, 24: 102–114

Yin, H. F., Jiang, H. S., Xia, W. C., et al., 2013. The End-Permian Regression in South China and Its Implication on Mass Extinction. *Earth Science Reviews*, 06: 003

Zhang, K. X., Lai, X. L., Ding, M. H., et al., 1995. Conodont Sequence and Its Global Correlation of P/T Boundary in Meishan Section, Changxing, Zhejiang Province. *Earth Sciences—Journal of China University of Geosciences*, 20(6): 669–678 (in Chinese with English Abstract)

Zhang, K. X., Lai, X. L., Tong, J. N., et al., 2009. Progresses on Study of Conodont Sequence for the GSSP Section at Meishan, Changxing, Zhejiang Province, South China. *Acta Palaeontologica Sinica*, 48(3): 474–486 (in Chinese with English Abstract)

Zhang, Y., Zhang, K. X., Shi, G. R., et al., 2014. Restudy of Conodont Biostratigraphy of the Permian-Triassic Boundary Section in Zhongzhai, Southwestern Guizhou Province, South China. *Journal of Asian Earth Sciences*, 80: 75–83

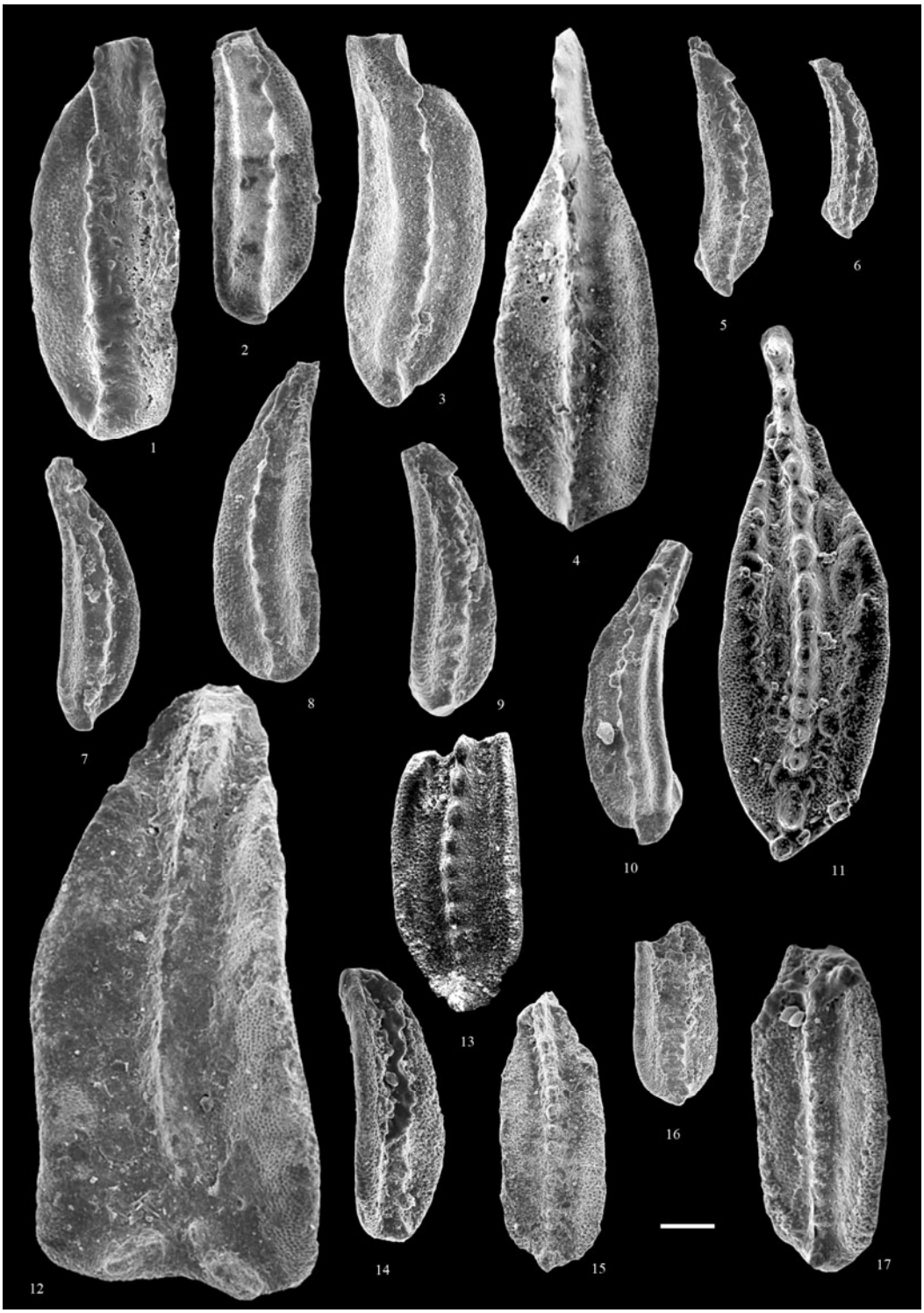

Plate 1. SEM photos of Permian conodonts. Scale bar equals to 100 μm. All specimens are housed in Faculty of Earth Sciences, China University of Geosciences, Wuhan. 1. *Clarkina wangi* (Zhang), lateral upper view, XM3-3/002. 2–10. *Clarkina changxingensis* (Wang and Wang); 2. lateral upper view, XM1-3/001; 3. lateral upper view, XM2-8/002; 4. upper view, XM3-3/001; 5. lateral upper view, XM5-1-2/046; 6. lateral upper view, XM5-1-2/101; 7. lateral upper view, XM5-1-2/088; 8. lateral upper view, XM5-1-2/037; 9. lateral upper view, XM5-1-2/008; 10. lateral upper view, XM5-3-1/005. 11. *Clarkina postwangi* (Tian), upper view, XM2-10/001. 12. *Clarkina tulongensis* (Tian), upper view, XM5-1-2/072. 13. *Clarkina yini* Mei, upper view, XM4-3/002. 14–17. *Clarkina meishanensis* Zhang, Lai, Ding, Wu and Liu; 14. lateral upper view, XM5-1-2/077; 15. upper view, XM5-1-2/097; 16. lateral upper view, XM5-1-2/142; 17. upper view, XM5-3-1/012.

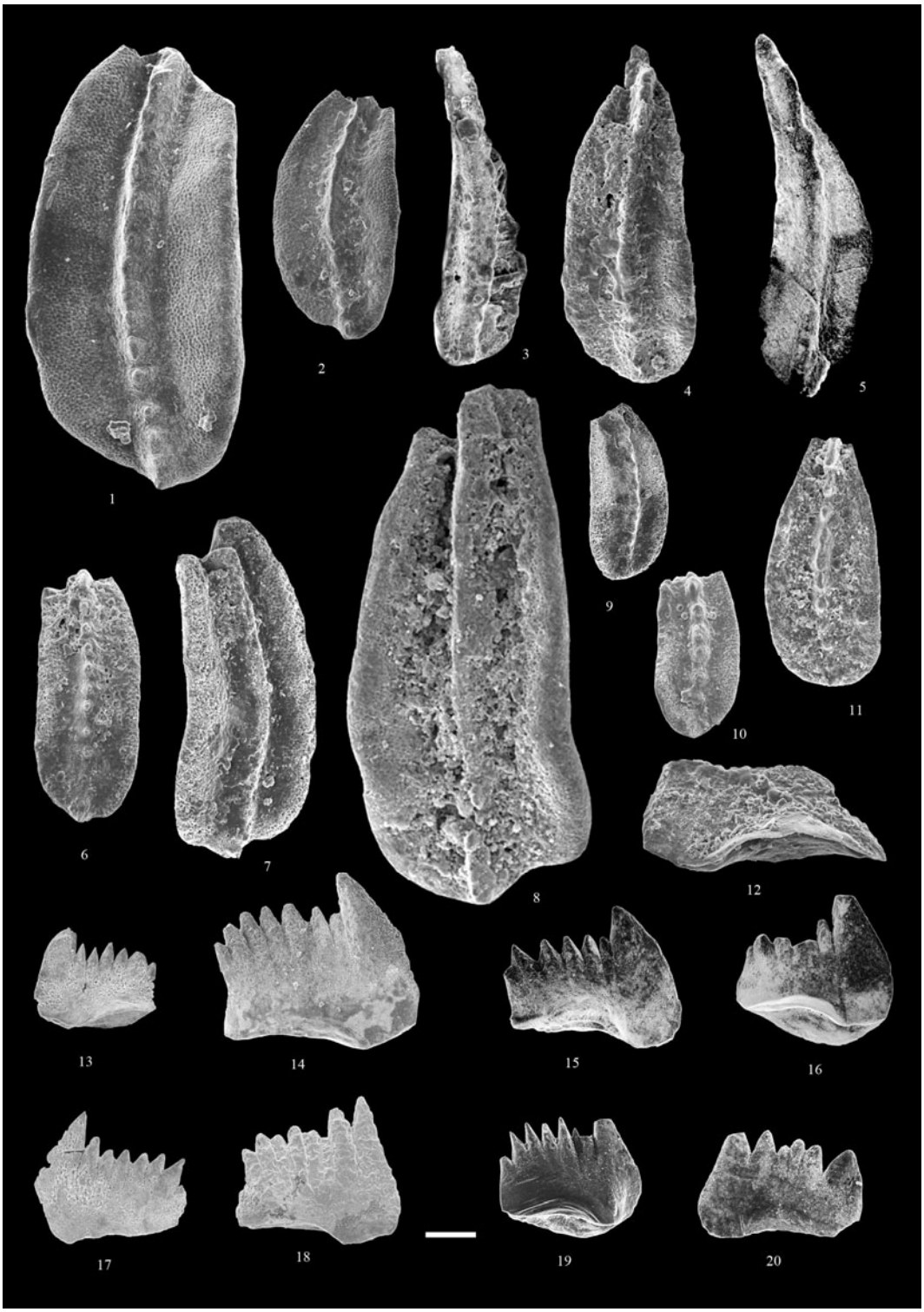

Plate 2. SEM photos of Permian-Triassic conodonts. Scale bar equals to 100 μm. All specimens are housed in Faculty of Earth Sciences, China University of Geosciences, Wuhan. 1–2. *Clarkina* sp. *A* (Jiang); 1. lateral upper view, XM5-1-2/122; 2. upper view, XM5-3-1/002. 3-11. *Clarkina* spp.; 3. lateral upper view, XM3-3/003; 4. upper view, XM4-3/001; 5. lateral upper view, XM5-3-1/003; 6. upper view, XM5-1-2/054; 7. lateral upper view, XM5-1-2/113; 8. upper view, XM5-1-2/068; 9. upper view, XM5-1-2/108; 10. upper view, XM5-1-2/161; 11. upper view, XM5-1-2/129. 12. *Hindeodus changxingensis* Wang, lateral view, XM5-3-1/007. 13–16. *Hindeodus parvus* (Kozur and Pjatakova), lateral view; 13. XM5-3-3/B_001; 14. XM5-3-4/B_002; 15. XM5-3-4/B_003; 16. XM5-3-4/B_004. 17–18. *Hindeodus praeparvus* (Kozur), lateral view; 17. XM5-3-4/B_005; 18. XM5-3-4/B_006. 19–20. *Hindeodus* spp., lateral view; 19. XM5-3-4/B_007; 20. XM5-3-4/B_008.